Received: 26 October 2021 | Revised: 1 December 2021 | Accepted: 7 December 2021

DOI: 10.1096/fba.2021-00130

FASEB BioAdvances WILEY

RESEARCH ARTICLE

Growth arrest of PPP2R5C and PPP2R5D double knockout mice indicates a genetic interaction and conserved function for these PP2A B subunits

Jade J. Dyson | **Fatima Abbasi** | **Prajakta Varadkar** | **Brent McCright**

FDA, Center for Biologics Evaluation and Research, Silver Spring, Maryland, USA

Correspondence
Brent McCright, FDA, Center for Biologics Evaluation and Research, 10903 New Hampshire Avenue, Building 52, Room 3210, Silver Spring, MD, USA.
Email: brenton.mccright@fda.hhs.gov

Abstract

Protein phosphatase 2A (PP2A) is a heterotrimeric phosphatase that controls a wide range of cellular functions. The catalytic activity and intracellular location of PP2A are modulated by its association with regulatory B subunits, including B56 proteins, which are encoded by five separate genes in humans and mice. The specific effects of each B56 protein on PP2A activity and function are largely unknown. As part of an effort to identify specific PP2A–B56 functions, we created knockout strains of B56β, B56δ, and B56ε using CRISPR/Cas9n. We found that none of the individual B56 genes are essential for mouse survival. However, mice that have both B56δ and B56γ inactivated (B56δγ−), arrest fetal development around Day E12. The hearts of B56δγ- mice have a single outflow vessel rather than having both an aorta and a pulmonary artery. Thus, there appears to be strong genetic interaction between B56δ and B56γ, and together they are necessary for heart development. Of note, both these proteins have been shown to localize to the nucleus and have the most related peptide sequences of the B56 family members. Our results suggest there are B56 subfamilies, which work in conjunction to regulate specific PP2A functions.

KEYWORDS

B56, heart development, PP2A, protein phosphatase 2A, regulatory B subunit

1 | INTRODUCTION

PP2A plays a role in controlling many essential cellular functions including DNA replication, cell cycle progression, mitosis, and signal transduction. PP2A exists primarily as a heterotrimeric complex consisting of a 30 kDa catalytic C subunit, a 65 kDa scaffold A subunit, and a variable regulatory B subunit. There are four multimember families of PP2A regulatory B subunits, identified as B/PR55/PPP2R2, B'/B56/PR61/PPP2R5, B''/PR72/PPP2R3, and striatins.[1,2] The B56 regulatory B subunits, the focus of this study, have

Abbreviations: Cas9n, nickase version of Cas9 nuclease; CRISPR, clustered regularly interspaced short palindromic repeats; E12, embryos 12 days after fertilization; Indel, Insertion–deletion; MEFs, mouse embryonic fibroblasts; PP2A, Protein phosphatase 2A; sgRNA, single guide RNA.

multiple naturally occurring splice variants and are encoded by five genes in mammals.[3–5] B56 is highly conserved, and the five genes appear to have been generated through a series of gene duplications, followed by genetic drift. In *Saccharomyces cerevisiae*, there is only one gene for B56, Rts1. In *Drosophila melanogaster* there are two B56 genes––*widerborst* and *well-rounded*, and in *Caenorhabditis elegans* there also two genes for B56, *pptr-1* and *pptr-2*. Mammalian B56γ and B56δ proteins are most related to Well-rounded and PPTR-2, while B56α, B56β, and B56ε peptide sequences are most similar to Widerborst and PPTR-1 (Figure 1).

PP2A containing B56 regulatory subunits (PP2A–B56) have been identified as having significant roles in the control of chromosome congression, chromosome distribution, and the spindle assembly checkpoint (SAC).[6] PP2A–B56 has been detected at the kinetochore during mitosis using GFP-A subunit and GFP-B56 fusion proteins, and B56 siRNA treatment was found to result in misaligned chromosomes.[7] The localization of PP2A to kinetochores depends on its interactions with BubR1[8] and Shugoshin-1 (Sgo1).[9] PP2A, in association with its B56γ regulatory subunit, has been shown to be needed for the stability of BubR1 during nocodazole-induced cell cycle arrest.[10] In primary cells that lacked B56γ, BubR1 was prematurely degraded and the cells proceeded through mitosis. The reduced SAC efficiency results in cells with abnormal chromosomal segregation, a hallmark of transformed cells. In other studies, the absence of the PP2A–B56 BubR1 interaction, resulted in aneuploidy, similar to that observed in Mosaic Variegated Aneuploidy syndrome cell lines.[11]

B56 family members are expressed during embryonic development and have been shown to influence the Wnt/β-catenin signaling pathway, which plays a major role in controlling organogenesis.[12–14] PP2A–B56 activity has also been shown to play a role in regulating insulin signaling and lipid metabolism via the regulation of Akt phosphorylation in both *C. elegans*[15] and *Drosophila*.[16]

Mutations in B56β, B56γ, and B56δ have been found in patients with overgrowth syndrome, a heterogeneous disorder characterized by excessive growth parameters, often in association with intellectual disability.[17] Mutations in B56δ have also been shown to be associated with intellectual disability and neurodevelopmental delay.[18] These B56δ mutations are autosomal dominant and are believed to mainly occur due to de novo mutations. The mechanism behind these neurological abnormalities is unknown.

Prior studies have reported phenotypes in mice that have B56α, B56γ, and B56δ inactivated. Consistent with the important role of PP2A–B56 interactions in regulating mitosis and cell cycle progression, inactivation of B56α and B56δ has been associated with oncogenesis in mice. B56α gene trapped mice develop skin lesions[19] and B56δ mice also develop tumors, both primarily in older mice.[20] Mice that have B56γ inactivated via a gene trap, have heart development and coordination abnormalities.[21] B56δ mutations have also been shown to cause coordination abnormalities.[22]

In this study, we used CRISPR/Cas9n to inactivate B56β and B56ε and present the first report on the phenotypes of these knockout mice. The B56β and B56ε knockout mice were viable and thus, taken with the information presented above, none of the five B56 genes are essential

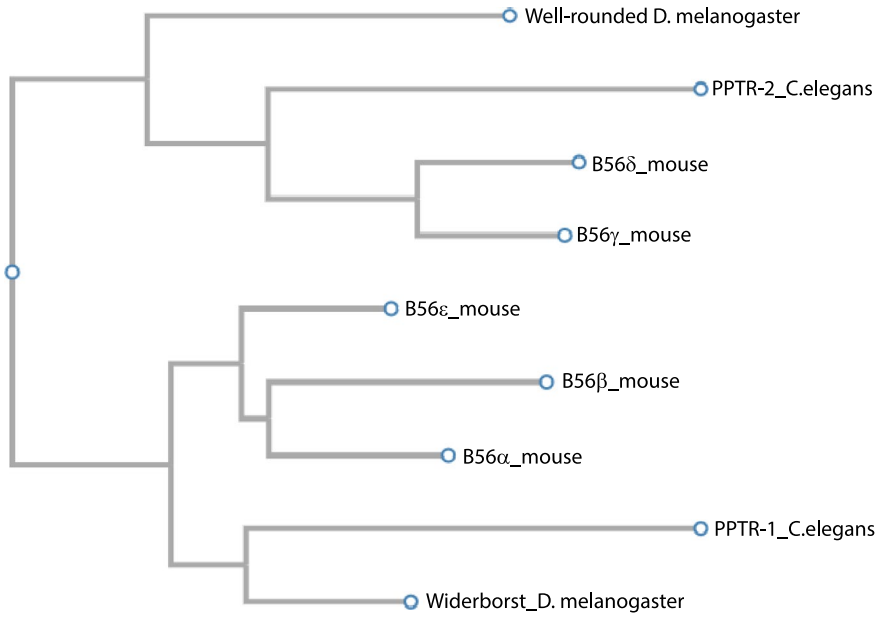

FIGURE 1 B56 peptide similarity. This dendrogram is generated using CLUSTALW https://www.genome.jp/tools-bin/clustalw. Eukaryotic B56s segregate into two families based on peptide similarity. B56α, B56β, and B56ε are more related to Widerborst and PPTR-1, while B56γ and B56δ are more related to Well-rounded and PPTR-2

for embryonic and adult survival. This is likely due to functional redundancy among the B56 genes. To explore the functional relationships and test for genetic interactions between the B56 subunits, we created mice containing combinations of B56 knockouts. We have found a strong genetic interaction between B56δ and B56γ, the two mammalian B56 proteins most related to each other (Figure 1). Inactivation of both genes, in combination, results in embryonic lethality at mid-gestation and hearts having a single outflow vessel, indicating these two genes form a subgroup involved in a similar function.

2 | MATERIALS AND METHODS

2.1 | CRISPR-Cas9 mice

The double nickase approach was used to introduce indels into the 5' region of B56β, B56δ, and B56ε genes (Table 1,[23]).

Optimal B56β, B56δ, and B56ε sgRNA pairs were identified using the website at http://crispr.mit.edu/.

Oligos were used to make templates for T7 sgRNA synthesis.

CRRNA2	AAAAAAGCACCGACTCGGTGCCACTTTTTCAAGTTGATAACGGACTAGCCTTATTTTAACTTGCTATTTCTAGCTCTAAAAC
M2B56bc-1	TTAATACGACTCACTATAGG**TCTCCCGCAGGTCCCTCCGC**GTTTTAGAGCTAGAAATAGC
M2B56bc-2	TTAATACGACTCACTATAGG**CCATCCACCTTGTCTGGTGG**GTTTTAGAGCTAGAAATAGC
M2B56dc-1	TTAATACGACTCACTATAGG**ACTGTTGCTGGGTCGCTTGT**GTTTTAGAGCTAGAAATAGC
M2B56dc-2	TTAATACGACTCACTATAGG**CTCAGCAAAATCAAGTACTC**GTTTTAGAGCTAGAAATAGC
M2B56ec-3	TTAATACGACTCACTATAGG**AGTTTCTTTAGGAACAGTTC**GTTTTAGAGCTAGAAATAGC
M2B56ec-4	TTAATACGACTCACTATAGG**CTGTGTCATTTTTGACTTCA**GTTTTAGAGCTAGAAATAGC

Oligos were synthesized (Integrated DNA Technologies), purified, and a high-fidelity PCR polymerase (Thermo Fisher Scientific) was used to make the double-stranded DNA template for the sgRNA synthesis. The sgRNAs were made by T7 in vitro transcription from PCR extended oligo templates. mRNA coding for Cas9n was obtained from TriLink BioTechnologies. CRISPR sgRNAs and Cas9n mRNA were microinjected into C57BL/6 zygotes by the Johns Hopkins transgenic core facility to create B56β, B56δ, and B56ε mice that were chimeric for indels. Mice carrying the indels were identified using the Surveyor kit (IDT). DNA spanning the indel was amplified by PCR and sequenced to identify mice that carried indels that cause frame shifts and therefore would result in null alleles. The strains containing the indels were outcrossed to C57BL/6J mice at least three times before phenotypic analysis was begun.

2.2 | Gene trapped mice

Mice that contained a gene trap for B56α (IST3127C10) were obtained from the Texas A&M Institute for Genomic Medicine. Studies with these mice have been published by others.[19] Gene trapped embryonic stem cells for B56δ (RRT114) and B56ε (YHD256) were obtained from the Mutant Mouse Resource and Research Center (MMRRC). The gene trapped embryonic stem cells were injected into C57BL/6J blastocysts and chimeric mice were bred onto a C57BL/6J background.

2.3 | β-galactosidase staining

Embryos from timed matings were fixed in PFA for 1 h and then incubated in a solution containing 5 mM potassium ferricyanide, 5 mM potassium ferrocyanide, 2 mM magnesium chloride, and 1 mg/ml X-gal.

2.4 | Western blots

Brains from neonatal mice homozygous for B56β, B56δ, and B56ε indels and wild-type mice were used to make protein extracts. The protein extracts were separated by SDS-PAGE and transferred to nitrocellulose membranes for immunostaining. The primary antibody used to detect B56β was HPA036607 (Sigma Millipore), B56δ was HPA029046 (Sigma Millipore), and B56ε was MABS270 (Sigma Millipore).

2.5 | Mouse breeding for phenotypic analysis

B56ε and B56γ genes are both localized to chromosome 12, about 18 cm apart. To obtain double knockout mice, B56ε+/−; B56γ+/− mice were bred and genotyped to identify mice that had a recombination event placing both mutations on the same chromosome. These mice were then intercrossed for experiments.

TABLE 1 CRISPR-Cas9n-induced indels in B56 mice

	Allele name; indel size; expected type of mutation	Guide RNA target region
B56β	b68; 13bp deletion; null b79; 41bp deletion; null	Exon 2 (Genomic: bp 1101–1120; mRNA: bp 689–708) Exon 2 (Genomic: bp 1079–1098; mRNA: bp 667–686)
B56δ	d918a1; 17bp deletion; null d967; 52bp deletion; null	Exon 3 (Genomic: bp 4983–5002; mRNA: bp 286–305) Exon 3 (Genomic: bp 4945–4964; mRNA: bp 324–313)
B56ε	e38; 50bp deletion; null e49; 9bp deletion + 2bp insertion = 7 bp deletion; null	Exon 3 (Genomic: bp 80426–80445; mRNA: bp 754–773) Exon 3 (Genomic: bp 80455–80474; mRNA: bp 783–802)

For B56δ × B56γ experiments, mice were bred to obtain B56δ−/−; B56γ+/− mice. The B56δ−/−; B56γ+/− mice were then intercrossed to obtain B56δγ- mice, mice doubly homozygous for both B56δ and B56γ indels.

2.6 | Immunohistochemistry

Litters of E12 embryos were harvested and fixed 1–2 h in 4% PFA. The tissues were embedded in freezing media and cryosectioned at 7 uM. Anti-α-actinin (Sigma, A7811) was used to detect myocytes. Anti-smooth muscle actin (Sigma, C6198) was used to detect immature myocytes. Anti-CD31 (BD Pharmingen, Clone MEC13.3) was used to detect endothelial cells. To detect cleaved caspase-3 (Asp 175), antibody 9661 was obtained from Cell Signaling Technology. The number of caspase-3-positive cells per heart section was counted and an average and standard deviation were calculated.

2.7 | Cell cycle analysis

Mouse embryonic fibroblasts (MEFs) were obtained from E11 litters and cultured in media containing DMEM/glutamax, 10% FBS, nonessential amino acids, and pen/ strep. For analysis, MEFs were fixed in 70% ethanol at −20°C for 1 h. The MEFs were then stained using propidium iodide/ RNase solution (Cell Signaling). DNA content was then analyzed by flow cytometry using a FACSCanto II (Becton Dickinson).

3 | RESULTS

As a first step toward identifying the functional requirements for B56 subunits during mammalian development, we obtained and made B56α, B56δ, and B56ε mice containing gene trap reporters. The gene trap was designed to interrupt transcription of the target gene using a splice acceptor fused to the β-galactosidase gene. We used these mice to observe the expression of B56 genes during fetal development (Figure 2). B56α is primarily expressed in the heart and liver bud at E10. B56δ and B56ε are more widespread, with high expression in the developing nervous system, pharyngeal arches, and limb buds. B56δ is also expressed in the myocardium of the developing heart at E10.

To facilitate the identification of B56 functional redundance and genetic interaction, we were interested in making mice that had combinations of B56 genes inactivated. To create true null alleles in B56 genes for this purpose, we decided to use CRISPR-Cas9. A double nickase strategy using CRISPR-Cas9n was chosen to inactivate B56β, B56δ, and B56ε to minimize the chances of off-target deletions (Table 1, Materials and Methods,[23]).

To demonstrate that the indels produced by CRISPR/Cas9n cause null mutations, immunostaining of protein extracts from mice containing the various indels was conducted. As shown in Figure 3, CRISPR targeting resulted in no wild-type protein being expressed in mice containing indels that caused a frameshift. Since the targeted sites were all 5' of the sequence coding for the highly conserved region that binds to the A subunit of PP2A, it is likely that these are true functional null mutations of the B56 genes. For our phenotypic analysis of the B56 CRISPR-Cas9n mice, we examined mice that contain the two independent indels as shown in Table 1 for each gene we targeted.

Mice homozygous for B56β indels were maintained until they were over 1.5 years old, during which no overt developmental defects were observed. Likewise, no phenotypic abnormalities were observed in mice homozygous for B56δ indels.

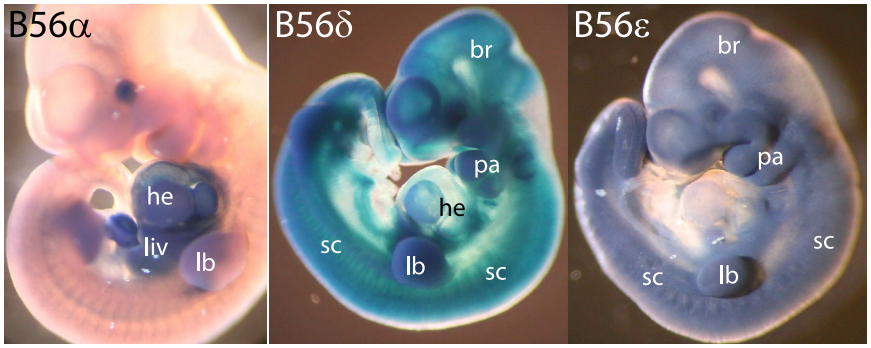

FIGURE 2 Expression of B56 genes during fetal development. Embryos containing B56α, B56δ, and B56ε gene trapped β-galactosidase reporters are taken at gestation day 10 (E10) and then stained using X-gal. B56α is primarily expressed in the heart, liver bud, and limb buds at E10 (he, liv, lb). B56δ and B56ε have a high amount of expression in the developing nervous system including the spinal cord (sc) and brain (br). B56δ and B56ε are highly expressed in the limb buds (lb) and pharyngeal arches (pa). B56δ is also expressed in the myocardium of the developing heart (he)

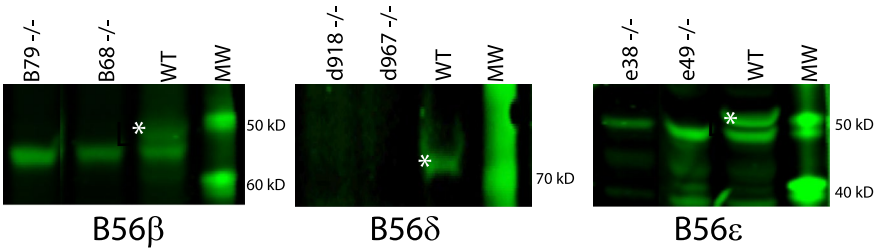

FIGURE 3 Western blots of protein extracts from wild type and mice that have indels created using CRISPR-Cas9n. Antibodies specific for B56β, B56δ, and B56ε are used for detection of the native B56 proteins by western blot. No B56 protein is detected in mice homozygous (−/−) for the B56β, B56δ, and B56ε indels. The B56β and B56ε antibodies cross reacted with a nonspecific protein. The asterisk (*) marks the wild-type protein present in the lanes associated with the wild-type protein extracts. MW = molecular weight markers

Mice homozygous for B56ε indels had a delay in neonatal growth and were noticeably smaller than their heterozygous and wild-type littermates (Figure 4A). However, after weaning, the homozygous B56ε mice grew to be similar in size to their littermates and were fertile. No phenotypic abnormalities were observed during gestation. Mice homozygous for the B56ε gene trap used for B56ε β-galactosidase expression analysis (Figure 2C), also exhibited delayed neonatal growth, similar to that observed in mice homozygous for the B56ε indels.

Since the knockouts of single B56 genes did not result in developmental arrest or death (Table 2), we assumed that there is functional redundancy among the B56 subunits. This functional redundancy could be based on multiple B56 genes being expressed in the same tissues and/or multiple B56 proteins being present in the same intracellular locations.

Previously, we reported that B56γ knockout mice had developmental defects in the heart that appeared during mid- and late-gestation.[21] Since B56α is highly expressed in the heart, we intercrossed B56γ and B56α knockout mice to see if they genetically interacted to result in a more severe heart phenotype. Mice that were homozygous for both gene traps, B56γ−/−; B56α−/− were very similar in appearance to the B56γ−/− mice, with ventricular septum defects and partial neonatal lethality (data not shown). Since the B56γ−/−; B56α−/− mice have similar phenotypes as the B56γ−/− mice, there does not appear to be substantial genetic interaction between B56α and B56γ.

Since B56ε and B56γ are most highly expressed in MEFs,[10] we created mice that had both of these genes inactivated, B56ε−/−; B56γ−/− (B56γε−). At E17, the hearts of B56γε- mice have a ventricular septation defect and the right ventricle is underdeveloped and triangular shaped (Figure 4). These heart abnormalities are similar, but slightly more pronounced than those observed previously in B56γ−/− mice.[21] The B56γε- mice are viable throughout gestation and are born at the expected Mendelian ratio, but they do not survive until weaning. In contrast, about half of B56γ−/− mice survive to adulthood. Since B56γε- mice do not survive to adulthood and have additive effects on heart development, these two genes appear to interact genetically and have some conserved biological functions.

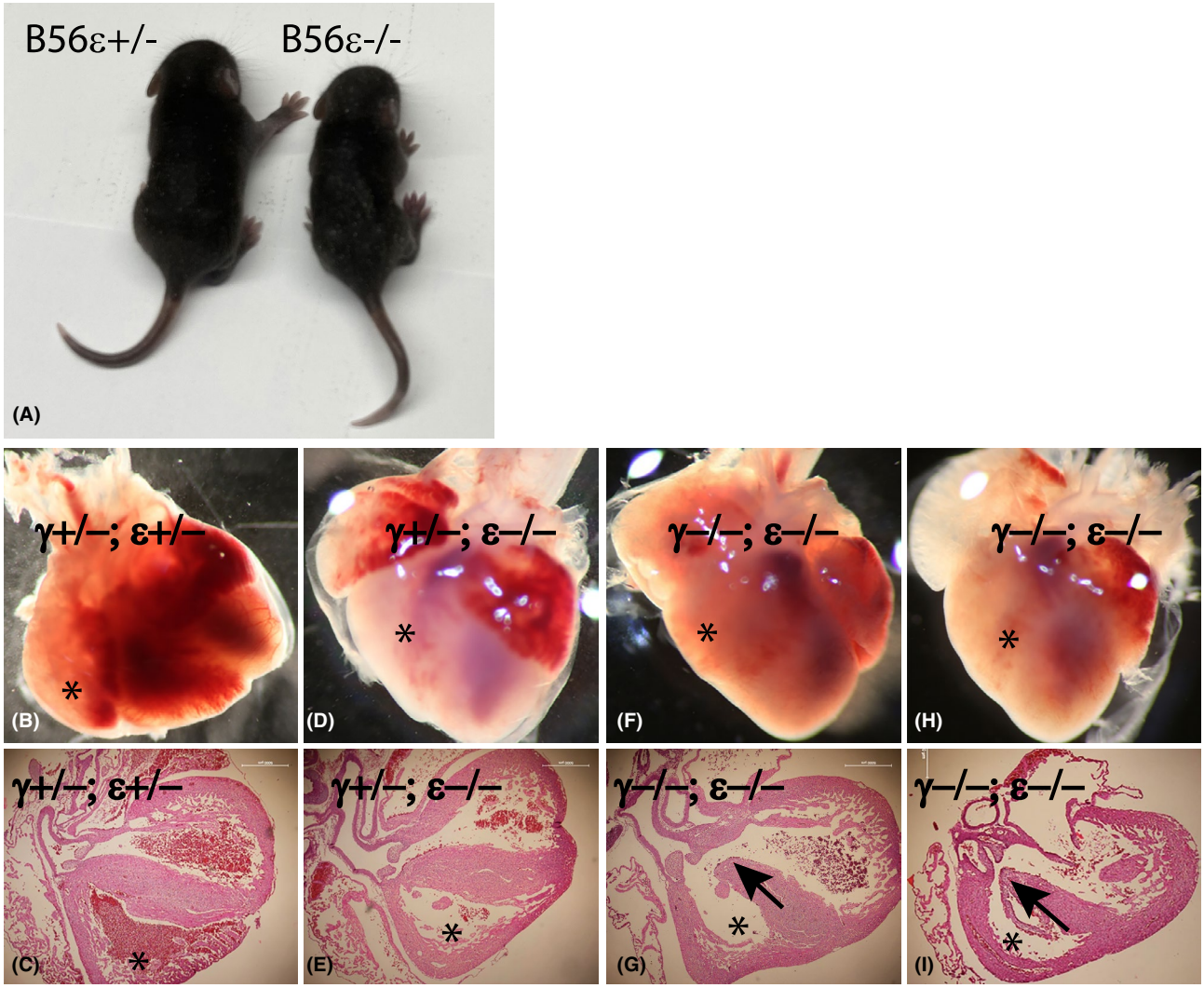

FIGURE 4 B56ε−/− neonates are smaller, histology of B56γε- hearts around Day 17 of gestation (E17). (A) Neonatal B56ε mice (right) are smaller than B56ε+/- littermates at 10 days old. Paraffin sections (C, E, G, and I) and whole hearts (B, D, F, and H) from E17 embryos doubly homozygous for B56γ and B56ε knockouts (F,G, H, and I) show hearts with ventricular septation defects (arrow) and a right ventricle that is underdeveloped and triangular shaped (*). Paraffin sections and whole hearts from E17 embryos that are doubly heterozygous (B and C) or heterozygous for B56γ and homozygous for the B56ε knockouts (D and E) do not have septation defects and have a more fully formed right ventricle (*)

Next, we made B56δ−/−; B56γ−/− (B56δγ−) mice that have both B56δ and B56γ knocked out, since B56δ and B56γ both localize to the nucleus and also have peptide sequences that are most related to each other.[24] This combination resulted in the arrest of development around Day E12 in 100% of the fetuses (Figure 5). The B56δγ− mice arrest heart development with a single outflow vessel rather than having both an aorta and a pulmonary artery. The developing limbs of the E14 B56δγ− mouse are underdeveloped relative to their littermates. No brain or neurological development defects were detected in B56δγ− fetuses during dissections or by histology (Figure 5). Since B56δγ− is embryonic lethal, there appears to be strong genetic interaction between B56δ and B56γ.

To determine if there were differences in cell types present in the B56δγ− hearts, we performed immunohistochemistry to determine if PP2A–B56δγ activity is needed for cell lineages present in the heart (Figure 6). By comparing B56δγ− hearts to their littermates, no major differences in myocardial, smooth muscle, or endothelial cell lineages were observed. Therefore, it does not appear that B56 participates in cell lineage specification in the heart.

Caspase-3 immunohistochemistry was performed on E12 hearts to determine if there are more apoptotic cells present in the B56δγ− embryos. We observed an increased number of caspase-3-positive cells in the B56δγ- hearts (average per heart section = 27.25, SD 6.67) relative to B56δγ−/+ hearts (average per heart section = 7.83, SD 2.13) indicating that there is an increased amount of apoptosis occurring

TABLE 2 Phenotypes of single B56 knockouts and double knockouts in combination with B56γ

	Single knockout phenotypes	Double Knockout (dKO) in combination with B56γ
B56α	No overt developmental defects	dKO, B56αγ- mice have similar phenotypes to B56γ- mice
B56β	No overt developmental defects	No dKO, B56βγ- mice have been made
B56δ	No overt developmental defects	dKO, B56δγ- mice arrest development at E12 with a single vessel outflow tract
B56ε	Neonatal B56ε- mice are smaller than littermates, adults are fertile and normal in appearance	dKO, B56γε- mice have a slightly stronger heart phenotype that B56γ- alone. B56γε- mice survive gestation but die perinatally.
B56γ	Fetal B56γ- mice have a heart ventricular defect. Neonates are smaller than littermates and half die before weaning. Adult B56γ- mice are uncoordinated.	

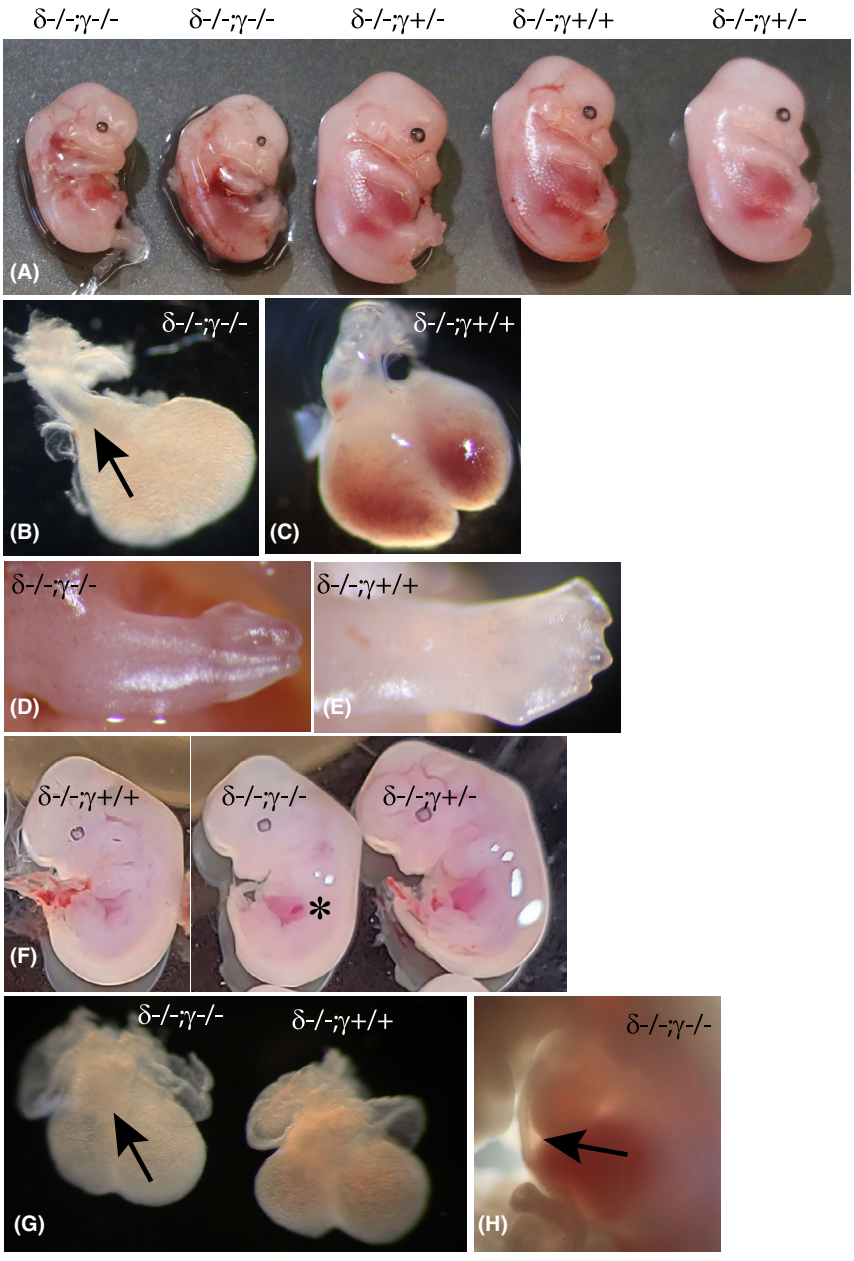

FIGURE 5 Inactivation B56δ and B56γ in combination causes an arrest of fetal development around Day E12. (A) The litter of E14 mice contains two B56δ−/−; B56γ−/− double knockout mice which are smaller than their B56δ−/−; B56γ+/- and B56δ−/−; B56γ+/+ littermates. The hearts of the double knockout mice contain a single outflow vessel (B, arrow) rather than having both an aorta and a pulmonary artery (C). The developing limbs of the E14 B56δ−/−; B56γ−/− mouse (D) also are underdeveloped relative to the B56δ−/−; B56γ+/+ littermate (E). At E12, there is not a noticeable size difference between the double knockout mouse and its littermates (F, *). The heart of the B56δ−/−; B56γ−/− E12 mouse has a single outflow vessel (G, arrow) and has pericardial edema (H, arrow)

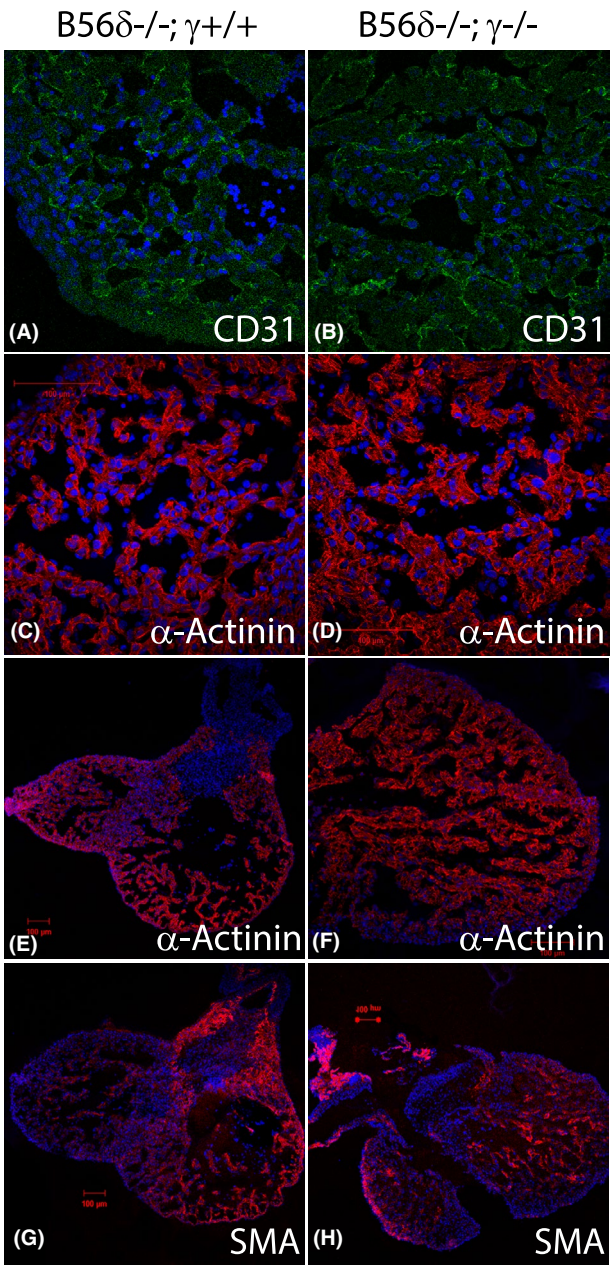

FIGURE 6 Immunohistochemistry of B56δ−/−; B56γ−/− hearts at E12. (A and B) An antibody to CD31 is used to detect endothelial cells (green) in B56δ−/−; B56γ−/− (B) and B56δ−/−; B56γ+/+ (A) E12 hearts. An antibody to α-actinin (red) is used to detect myocytes in B56δ−/−; B56γ−/− (D, F) and B56δ−/−; B56γ+/+ (C, E) E12 hearts. An antibody to smooth muscle actin (SMA, red) is to detect smooth muscle cells and immature myocytes in B56δ−/−; B56γ−/− (H) and B56δ−/−; B56γ+/+ (G) E12 hearts

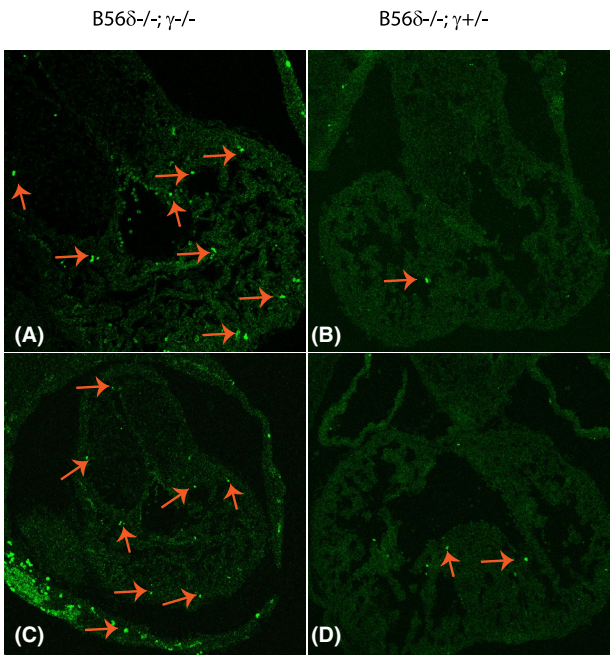

FIGURE 7 Caspase-3 immunohistochemistry. Caspase-3 immunohistochemistry is used to detect apoptotic cells in E12 B56δ−/−; B56γ−/− hearts (A and C), and B56δ−/−; B56γ+/- hearts (B and D). Caspase-3-positive cells are seen in the B56δ−/−; B56γ−/− hearts (A, C, highlighted with arrows)

(Figure 7). This coincides with the apparent arrest in heart development and embryonic death that occurs around E12.

The lack of a cell lineage defect and the presence of widespread cell death suggested that there may be a cell growth problem intrinsic to B56δγ- cells. Therefore, E11 embryonic fibroblasts (MEFs) were isolated from the B56δγ- fetuses and littermates to look for abnormalities in cell growth. Using standard MEF isolation procedures, approximately 2- to 3-fold fewer cells were obtained from the B56δγ− fetuses than fetuses of other genotypes. In addition, the B56δγ- MEFs could not be expanded in culture to the extent cells that non-B56δγ− MEFs were expanded. Cell cycle analysis of MEFs using propidium iodide staining and flow cytometry indicates there is a larger population of B56δγ- cells in G2/M phase compared to other genotypes (Figure 8). Thus, it appears there is a delay in B56δγ- cells proceeding through mitosis.

4 | DISCUSSION

Since the amino acid sequences of the proteins encoded by the five B56 genes are highly conserved, it is likely that there is some level of functional redundancy between the B56 family members. However, how much redundancy is still an open question. Previous studies have indicated that B56 subunits localize to different regions of the cell, which would support the hypothesis that the B56 family members could have functions unique to specific subunits.[10,24] Another argument against complete functional redundancy, are the findings that single gene B56 mutations have been found to be associated with oncogenesis.[19,20] Since multiple B56 genes are expressed in most tissues,

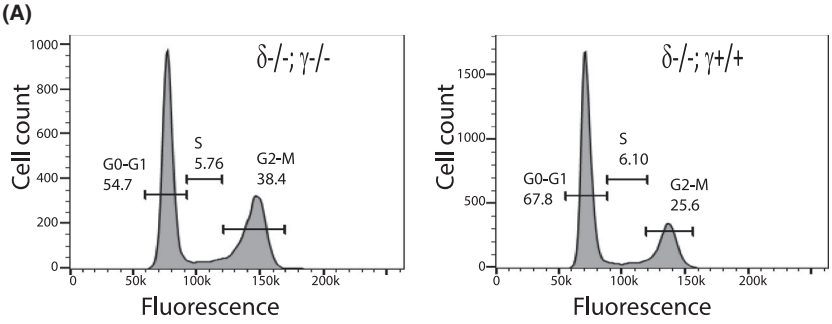

FIGURE 8 Cell cycle analysis of mouse embryonic fibroblasts (MEFs). Embryonic fibroblasts isolated from B56δ−/−; B56γ−/− mice and littermates are stained with propidium iodide and then analyzed for DNA content using flow cytometry. (A) Shows representative data collected from B56δ−/−; B56γ−/− MEFs (left) and B56δ−/−; B56γ+/+ MEFs (right). The average G2/M content from multiple experiments is shown in (B)

(B)

	δ-/-; γ-/-	δ-/-; γ+/-	δ-/-; γ+/+	δ+/+; γ-/-	Wild type
Percentage of cells in G2/M	33.66 SD = 6.83	25.54 SD = 5.53	23.96 SD = 5.80	27.75 SD = 2.75	24.2 SD = 2.84

a single mutation could be compensated for by the other four B56 genes if they were all functionally redundant.

In this paper, we tested if other B56 subunits could genetically interact with B56γ by making mice that were doubly homozygous for two B56 genes (Table 2). If genetic interaction occurs, then this would be an indication that these genes are functionally redundant. In other words, if we uncover new phenotypes when two B56 genes are knocked out, then this would be evidence that those two genes are functionally redundant. Our first inquiry into functional redundancy with B56α and B56γ, was based on gene expression. Since B56α is expressed highly in the heart, we made B56αγ- mice with the expectation that we would see a stronger heart phenotype than what we saw with the B56γ− mouse. We did not, indicating that B56α and B56γ are likely not functionally redundant. Since B56ε and B56γ are the two B56 genes mostly highly expressed in MEFs, we next made B56γε− mice. Some genetic interaction was detected based on an increase in the severity of the heart septation defect and an increase in neonatal lethality. In contrast, B56γ genetically interacted with B56δ very strongly, even though B56δ is only moderately expressed in the heart and MEFs (Figure 2). We hypothesize that this is due to the conserved activity and function that these proteins confer to PP2A. These two genes are most similar in peptide sequence to each other and both B56γ and B56δ have been shown to localize to the nucleus. Based on peptide sequence, these two genes constitute a mammalian B56 subfamily, which is most similar to the *Drosophila melanogaster Well-rounded* and *Caenorhabditis elegans* PPTR-2 (Figure 1).

Investigators studying the function of PP2A and its regulation by B56 in vitro, have found that using siRNA against all five genes is an effective way to study the role of PP2A in regulating mitosis.[7] This approach is useful when studying specific cell features––it is easier to knockout as much of B56 activity as possible to allow a better readout. However, our results support the hypothesis that different B56 proteins have different functional capabilities in vivo. Therefore, it would be interesting to perform in vitro studies with subsets of siRNA oligos or use CRISPR/Cas9 to inactivate subsets of B56 genes to see if PP2A activity toward specific substrates is determined by B56 subfamilies. For instance, B56γ and B56δ could be inactivated and phosphorylation status of proteins could be compared to that observed with inactivation of B56α, B56β, and B56ε.

In our study, we found that knocking out B56γ and B56δ in combination, arrested mouse development at around Day 12 of gestation. The mice had a single outflow vessel instead of an aorta and a pulmonary artery. Septation of the single outflow vessel occurs around E11, so this result is consistent with there being a developmental problem with the heart, which in turn leads to death of the mouse. However, we could not detect any cell lineage abnormalities in the B56δγ− heart, and cells obtained from noncardiac tissue also displayed growth and cell cycle abnormalities. Therefore, we hypothesize that knocking out the combination of B56γ and B56δ causes proliferation problems in multiple cell types due to a PP2A–B56γ/δ activity needed for efficient progression through mitosis as evidenced by the higher percentage of MEFs present in G2/M phase.

Human intellectual disabilities have been associated with B56δ mutations and mutations in the PP2A catalytic subunit that affect B56 binding.[18,25] Interestingly, sensorimotor deficiencies have also been reported in B56δ[22] and B56γ[21] knockout mice. Therefore, these and other transgenic B56 mice may be useful for investigating and providing models for the growing number of neurological human diseases associated with mutations in PP2A genes. Inactivating PP2A–B56 subunits in mice via germline modification can identify functional requirements for PP2A during development but these studies are limited when the genetic modifications result in fetal lethality. However, a more targeted approach to gene inactivation using cell lineage-specific conditional knockouts would allow the study of PP2A–B56 function in juvenile and

adult mouse brains. Alternatively, transgenic mice can be used as sources of cells for studies aimed at understanding the regulation of PP2A activity in vitro. Findings from future transgenic mouse studies will likely be informative for both understanding normal PP2A function and provide information related to controlling growth in cancerous cells.

ACKNOWLEDGMENT

Funding for this work was obtained from the FDA, Center for Biologics Evaluation and Research.

CONFLICT OF INTEREST

The authors have no conflict of interest to declare.

AUTHOR CONTRIBUTIONS

B. McCright and J. J. Dyson designed the research. J. J Dyson, P. Varadkar, and F. Abbasi performed the research. J. J. Dyson, F. Abbasi, and B. McCright analyzed the data. J. J. Dyson, P. Varadkar, and B. McCright wrote the paper.

ORCID

Brent McCright https://orcid.org/0000-0001-6739-863X

REFERENCES

1. Shi Y. Serine/threonine phosphatases: mechanism through structure. *Cell*. 2009;139(3):468-484.
2. Virshup DM, Shenolikar S. From promiscuity to precision: protein phosphatases get a makeover. *Mol Cell*. 2009;33(5):537-545.
3. McCright B, Virshup DM. Identification of a new family of protein phosphatase 2A regulatory subunits. *J Biol Chem*. 1995;270(44):26123-26128.
4. Csortos C, Zolnierowicz S, Bako E, Durbin SD, DePaoli-Roach AA. High complexity in the expression of the B' subunit of protein phosphatase 2A0. Evidence for the existence of at least seven novel isoforms. *J Biol Chem*. 1996;271(5):2578-2588.
5. Tehrani MA, Mumby MC, Kamibayashi C. Identification of a novel protein phosphatase 2A regulatory subunit highly expressed in muscle. *J Biol Chem*. 1996;271(9):5164-5170.
6. Garvanska DH, Nilsson J. Specificity determinants of phosphoprotein phosphatases controlling kinetochore functions. *Essays Biochem*. 2020;64(2):325-336.
7. Foley EA, Maldonado M, Kapoor TM. Formation of stable attachments between kinetochores and microtubules depends on the B56-PP2A phosphatase. *Nat Cell Biol*. 2011;13(10):1265-1271.
8. Kruse T, Zhang G, Larsen MS, et al. Direct binding between BubR1 and B56-PP2A phosphatase complexes regulate mitotic progression. *J Cell Sci*. 2013;126(Pt 5):1086-1092.
9. Meppelink A, Kabeche L, Vromans MJ, Compton DA, Lens SM. Shugoshin-1 balances Aurora B kinase activity via PP2A to promote chromosome bi-orientation. *Cell Rep*. 2015;11(4):508-515.
10. Varadkar P, Abbasi F, Takeda K, Dyson JJ, McCright B. PP2A-B56gamma is required for an efficient spindle assembly checkpoint. *Cell Cycle*. 2017;16(12):1210-1219.
11. Xu P, Raetz EA, Kitagawa M, Virshup DM, Lee SH. BUBR1 recruits PP2A via the B56 family of targeting subunits to promote chromosome congression. *Biol Open*. 2013;2(5):479-486.
12. Seeling JM, Miller JR, Gil R, Moon RT, White R, Virshup DM. Regulation of beta-catenin signaling by the B56 subunit of protein phosphatase 2A 4. *Science (New York, NY)*. 1999;283(5410):2089-2091.
13. Martens E, Stevens I, Janssens V, et al. Genomic organisation, chromosomal localisation tissue distribution and developmental regulation of the PR61/B' regulatory subunits of protein phosphatase 2A in mice. *J Mol Biol*. 2004;336(4):971-986.
14. Li X, Yost HJ, Virshup DM, Seeling JM. Protein phosphatase 2A and its B56 regulatory subunit inhibit Wnt signaling in Xenopus. *EMBO J*. 2001;20(15):4122-4131.
15. Padmanabhan S, Mukhopadhyay A, Narasimhan SD, Tesz G, Czech MP, Tissenbaum HA. A PP2A regulatory subunit regulates C. elegans insulin/IGF-1 signaling by modulating AKT-1 phosphorylation. *Cell*. 2009;136(5):939-951.
16. Vereshchagina N, Ramel MC, Bitoun E, Wilson C. The protein phosphatase PP2A-B' subunit Widerborst is a negative regulator of cytoplasmic activated Akt and lipid metabolism in Drosophila. *J Cell Sci*. 2008;121(Pt 20):3383-3392.
17. Loveday C, Tatton-Brown K, Clarke M, et al. Mutations in the PP2A regulatory subunit B family genes PPP2R5B, PPP2R5C and PPP2R5D cause human overgrowth. *Hum Mol Genet*. 2015;24(17):4775-4779.
18. Biswas D, Cary W, Nolta JA. PPP2R5D-related intellectual disability and neurodevelopmental delay: a review of the current understanding of the genetics and biochemical basis of the disorder. *Int J Mol Sci*. 2020;21(4):1286.
19. Janghorban M, Langer EM, Wang X, et al. The tumor suppressor phosphatase PP2A-B56alpha regulates stemness and promotes the initiation of malignancies in a novel murine model. *PLoS One*. 2017;12(11):e0188910.
20. Lambrecht C, Libbrecht L, Sagaert X, et al. Loss of protein phosphatase 2A regulatory subunit B56delta promotes spontaneous tumorigenesis in vivo. *Oncogene*. 2018;37(4):544-552.
21. Varadkar P, Despres D, Kraman M, et al. The protein phosphatase 2A B56gamma regulatory subunit is required for heart development. *Dev Dyn*. 2014;243(6):778-790.
22. Louis JV, Martens E, Borghgraef P, et al. Mice lacking phosphatase PP2A subunit PR61/B'delta (Ppp2r5d) develop spatially restricted tauopathy by deregulation of CDK5 and GSK3beta. *Proc Natl Acad Sci USA*. 2011;108(17):6957-6962.
23. Ran FA, Hsu PD, Lin CY, et al. Double nicking by RNA-guided CRISPR Cas9 for enhanced genome editing specificity. *Cell*. 2013;154(6):1380-1389.
24. McCright B, Rivers AM, Audlin S, Virshup DM. The B56 family of protein phosphatase 2A (PP2A) regulatory subunits encodes differentiation-induced phosphoproteins that target PP2A to both nucleus and cytoplasm. *J Biol Chem*. 1996;271(36):22081-22089.
25. Reynhout S, Jansen S, Haesen D, et al. De novo mutations affecting the catalytic calpha subunit of PP2A, PPP2CA, cause syndromic intellectual disability resembling other PP2A-related neurodevelopmental disorders. *Am J Hum Genet*. 2019;104(2):357.

How to cite this article: Dyson JJ, Abbasi F, Varadkar P, McCright B. Growth arrest of PPP2R5C and PPP2R5D double knockout mice indicates a genetic interaction and conserved function for these PP2A B subunits. *FASEB BioAdvances*. 2022;4:273-282. doi:10.1096/fba.2021-00130